Chemodynamics of Metal Complexation by Natural Soft Colloids: Cu(II) Binding by Humic Acid

ARTICLE *in* THE JOURNAL OF PHYSICAL CHEMISTRY A · MARCH 2012

Impact Factor: 2.69 · DOI: 10.1021/jp212226j · Source: PubMed

THE JOURNAL OF PHYSICAL CHEMISTRY A

Article

pubs.acs.org/JPCA

Chemodynamics of Metal Complexation by Natural Soft Colloids: Cu(II) Binding by Humic Acid

Raewyn M. Town,*[,†] Jérôme F. L. Duval,[‡] Jacques Buffle,[§] and Herman P. van Leeuwen[⊥]

[†]Institute for Physics, Chemistry and Pharmacy, University of Southern Denmark, Campusvej 55, 5230 Odense, Denmark

[‡]Laboratoire Environnement et Minéralurgie, Nancy-University, CNRS UMR 7569, 15 avenue du Charmois, B.P. 40, 54501 Vandoeuvre-lès-Nancy Cedex, France

[§]CABE, Section de Chimie, University of Geneva, Sciences II, Quai Ernest-Ansermet 30, CH-1211 Geneva 4, Switzerland

[⊥]Laboratory of Physical Chemistry and Colloid Science, Wageningen University, Dreijenplein 6, 6703 HB Wageningen, The Netherlands

Supporting Information

ABSTRACT: The chemodynamics of Cu(II) complexation by humic acid is interpreted in terms of recently developed theory for permeable charged nanoparticles. Two opposing electric effects are operational with respect to the overall rate of association, namely, (i) the conductive enhancement of the diffusion of Cu^{2+}, expressed by a coefficient f_{el}, which accounts for the accelerating effect of the negative electrostatic field of the humic particle on the diffusive transport of metal ions toward it, and (ii) the ionic Boltzmann equilibration with the bulk solution, expressed by a factor f_B, which quantifies the extent to which Cu^{2+} ions accumulate in the negatively charged particle body. These effects are combined in the probability of outer-sphere metal−site complex formation and the covalent binding of the metal ion by the complexing site (inner-sphere complex formation) as in the classical Eigen mechanism. Overall "experimental" rate constants for CuHA complex formation, k_a, are derived from measurements of the thermodynamic stability constant, K^*, and the dissociation rate constant, k_d^*, as a function of the degree of metal ion complexation, θ. The resulting k_a values are found to be practically independent of θ. They are also compared to theoretical values; at an ionic strength of 0.1 mol dm^{-3}, the rate of diffusive supply of metal ions toward the particles is comparable to the rate of inner-sphere complex formation, indicating that both processes are significant for the observed overall rate. As the ionic strength decreases, the rate of diffusive supply becomes the predominant rate-limiting process, in contrast with the general assumption made for complexes with small ligands that inner-sphere dehydration is the rate-limiting step. The results presented herein also resolve the discrepancy between experimentally observed and predicted dissociation rate constants based on the above assumption.

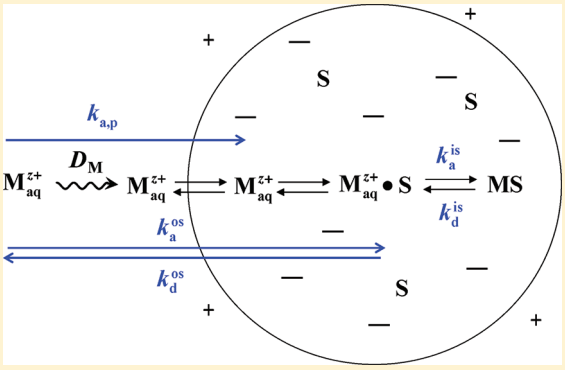

INTRODUCTION

Colloids or nanoparticles (NPs) are ubiquitous in environmental and biological media. They originate from both natural and engineered sources and are diverse in nature, ranging from soft and permeable to hard and compact. Knowledge of the chemodynamics of the interaction of NPs with ions and small molecules is fundamental to understanding and predicting their environmental impact. A defining feature of permeable NPs is that their sites are spatially confined inside of a particle body with an inner medium whose properties may be different from those of the bulk solution. The sites may comprise chemically reactive sites (either electrically charged or not) and, often, a larger number of non- or weakly complexing charged sites. Consequently, the features of the local complexation environment must be considered in the derivation and interpretation of kinetic parameters. The usual situation is that reported parameters such as the thermodynamic stability constant, K, and the rate constants for complex association, k_a, and dissociation, k_d, represent some sort of operational average for the entire particle dispersion.

It has recently been shown that for the case of soft nanoparticulate complexants, the Eigen mechanism applicable to aqueous metal ion complexation by simple ligands can be developed into a differentiated form.[1] In its original formulation, the Eigen scheme considers the complexation reaction as a two-step process; first, an outer-sphere reactant pair is formed, which is then followed by inner-sphere dehydration and complexation between the metal ion and the ligand. In the case of metal complexation by NPs, however, several distinguishable steps are

Special Issue: Herman P. van Leeuwen Festschrift

Received: December 19, 2011
Revised: February 9, 2012
Published: February 11, 2012

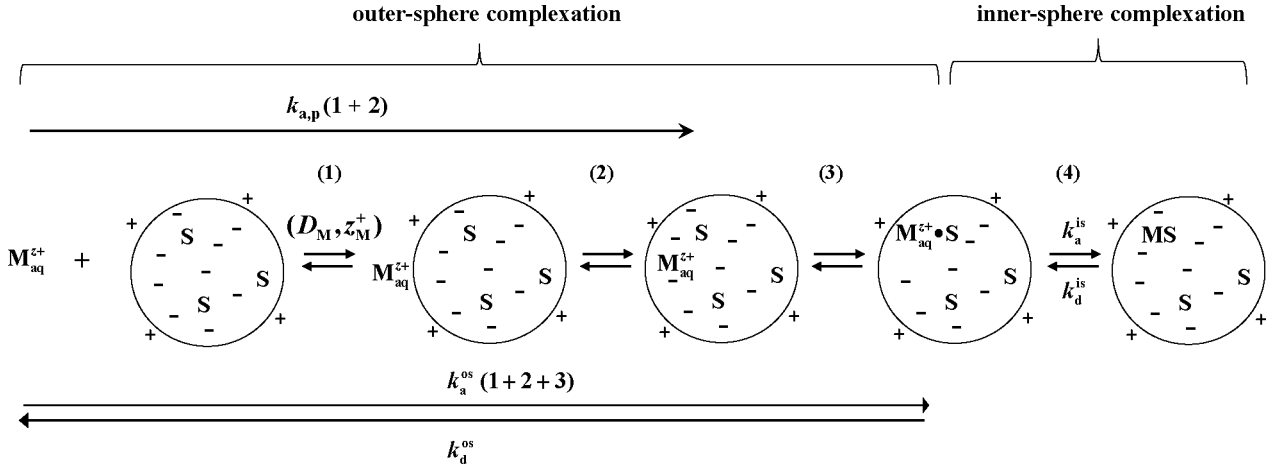

Figure 1. Stepwise complexation of a hydrated metal ion, M_{aq}^{z+}, with a nanoparticulate complexant containing charged or uncharged binding sites (S) and charged sites (−). The +'s denote the extraparticulate counterionic atmosphere. The steps are (1) diffusion of M_{aq}^{z+} from the bulk solution to the surface of the complexant, (2) crossing the solution/particle interface and incorporation within the particle as a free hydrated ion, (3) outer-sphere association of M_{aq}^{z+} with S, M_{aq}^{z+}·S, and (4) inner-sphere complex formation, MS, including the loss of water of hydration by M_{aq}^{z+} and formation of a chemical bond with site S.

involved in the overall complexation process, as illustrated in Figure 1. The particle size, the reactive site density, and the electric charge density play essential roles in determining the rates of the various component processes.

Any one of the steps outlined in Figure 1 may be rate-limiting. They depend on the nature of both the complexant (size, charge density, binding site density) and the type of metal ion (size, rate of dehydration, k_w). Here, we explore the nature of the rate-limiting step for Cu^{2+} complexation by a natural soft nanoparticle, humic acid (HA). The aqueous copper ion, $Cu(H_2O)_6^{2+}$, is chosen as a typical representative of metal ions with a high rate of dehydration ($k_w = 10^{9.6}$ s^{-1}),[2−5] thus featuring a relatively fast rate of inner-sphere complex formation. Accordingly, any process that limits the rate of outer-sphere reaction pair formation has the potential to be overall rate-limiting. At ambient pH, HA complexants carry a high negative charge density; thus, the electric field is likely to be significant in determining both the rate of metal ion diffusion toward and partitioning into the particle body. Here, we explore the magnitudes of these electric effects and elaborate on the consequences for chemodynamics of Cu−HA complexation.

A defining feature of HA is its chemical heterogeneity. This well-known characteristic has the consequence that the equilibrium relation between M and the various binding sites is given by a distributed affinity and an ensuing stability K, which varies with the degree of occupation of the binding sites, θ. In line with the Eigen mechanism, it has always been assumed that the association rate constant k_a is independent of θ, and thus, the distribution in K is reflected in that of the dissociation rate constant k_d.[6,7] Here, we shall explore the validity of this assumption for complexation between the negatively charged multisite ligand HA and the fast dehydrating metal ion Cu_{aq}^{2+}.

THEORY

The HA considered herein typically has a particle radius r_p of ∼2.3−3 nm, with approximately 30−50 carboxyl groups, which comprise the predominant charged sites at ambient pH.[8,9] The extraparticulate countercharge in the diffuse double layer in the solution is generally negligible with respect to the countercharge inside of the particle body.[10] The potential profile within the particle body is determined by the relative magnitude of the separation distance between the charged sites, l_S, as compared to the Debye screening length, κ^{-1}. The high charge density regime is characterized by $l_S \ll \kappa^{-1}$.[11] Assuming a homogeneous distribution of carboxyl groups within the HA particle volume, l_S is in the range of ∼1.2−1.9 nm (for r_p = 2.3−3 nm and 30−50 carboxyl groups). Thus, l_S/κ^{-1} is on order unity in the 0.01−0.1 mol dm^{-3} electrolyte concentration regime, implying that, for example, for fresh waters, these particles lie in the intermediate to high charge density regime.

It is less straightforward to specify the number and nature of the reactive sites. Potentially, all of the carboxyl groups may be involved in binding of Cu^{2+}, and other minor groups, for example, N- and S-containing functionalities may also contribute. The metal binding affinity of these various sites is distributed. Interpretation of the kinetic features for the heterogeneous multisite HA particles requires definition of the number of binding sites, N_S, per particle. For the simple case of N_S identical sites with identical binding strength, the total diffusive metal ion flux to the particle is shared among the sites. If, like in HA, the binding strength is dependent on the degree of site occupation, then the first metal ion encounters N_S identical sites, but for subsequent metal ions, the binding strength is lower (and the remaining available number of sites is lower). In the case of HA, however, the N_S sites are generally intrinsically different, leading to the overall affinity distribution applicable to the entire multiparticle dispersion. The first metal ion will be bound predominantly by the strongest site, that is, it spends relatively large amounts of time at the stronger site and smaller amounts of time at the weaker sites. This distribution will be of a Boltzmann type, and rigorous analysis requires a correspondingly weighted counting of the sites. At a given θ, part of the distribution may correspond to such low affinity sites that it is immaterial for metal ion binding (weighting factor → 0). For the present purposes, we exploit such individual site weighting as it is inherent in the differential equilibrium function, K^*, and the differential dissociation rate constant, k_d^*. As explained below, these functions are formulated so that at a given θ, the K^* or k_d^* tend to be representative of one particular type of reactive site.

Conductive Acceleration. The Smoluchowski−Debye approach[12,13] for ionic reaction rates combines an electric

dx.doi.org/10.1021/jp212226j | J. Phys. Chem. A 2012, 116, 6489−6496

force term with the diffusive flux equation for transport of M_{aq}^{z+} toward the charged simple ligand. The general solution for the conductive coefficient, f_{el}, in the diffusive flux incorporates an integral term involving the electrostatic energy between M_{aq}^{z+} and the ligand at a distance r, $U(r)$

$$f_{el} = \{r_L \int_{r_L}^{\infty} r^{-2} \exp(U(r)/k_B T)\, dr\}^{-1} \quad (1)$$

where r_L is the radius of the ligand.

By assuming that the electric force is of a purely Coulombic nature, with a $1/r^2$ dependence on the separation between the two charge centers, Debye found f_{el} to be[12]

$$f_{el} = \boldsymbol{U}/[\exp(\boldsymbol{U}) - 1] \quad (2)$$

where $\boldsymbol{U}$ is the dimensionless interaction energy between M_{aq}^{z+} and a simple ligand, given by

$$\boldsymbol{U} \approx z_M z_L e^2/(4\pi\varepsilon k_B T(r_L + r_M)) \quad (3)$$

where z_M and z_L are the charges of the metal ion and the ligand, respectively, and ε is the dielectric permittivity of the solution.

For $\boldsymbol{U} < 0$, the f_{el} (>1) represents the conductive accelerating effect of the negative electrostatic field on the diffusive transport of M_{aq}^{z+} toward the ligand.

The rate constant for the association between M_{aq}^{z+} and a charged nanoparticulate ligand is represented by $k_{a,p}$ in Figure 1. It has been expressed as a diffusive rate constant together with a coefficient for the conductive acceleration of the positively charged metal ion by the negative electrostatic field of the particle, f_{el}.[1] Accordingly, the diffusive flux expression yields for $k_{a,p}$

$$k_{a,p} = 4\pi N_{Av}(r_p + r_M)(D_M + D_p) f_{el} \quad (4)$$

where D_p is the diffusion coefficient of the particle and D_M is the diffusion coefficient of the metal ion. It has been recognized[1,14] that a Coulombic point charge approach is not rigorous for soft NPs, like HA, carrying charges spatially distributed throughout the particle volume. Recently, a new theory has been developed that rigorously describes the electrostatic force between a homogeneously charged nanoparticulate ligand and an approaching small ion.[14] The treatment quantifies the impact of the extra- and intraparticulate electrostatic field on the conductive diffusion process. The numerical evaluation of f_{el} for this ion/particle case is based on the nonlinear Poisson−Boltzmann equation considering a smeared-out distribution of charges. It allows for the computation of overall effective $\overline{f}_{el}$ values pertaining to the HA case, that is, values derived from the integral average of the local f_{el} over the position inside of the HA entity.[14]

Rate of Outer-Sphere Complex Formation. In the case of sufficiently large humics, the M_{aq}^{z+} generally fully enters the soft NP body. The outer-sphere complex formation process covers steps 1−3 in Figure 1. Thus, for the high charge density case, the relevant metal ion partitioning to consider is that between the outer-sphere volume V^{os} and the remaining particle volume, $V_p - N_S V^{os}$, where $V^{os} = (4/3)\pi a^3$, and a is the center-to-center distance between reactants in the outer-sphere reactant pair. When $N_S V^{os} \ll V_p$, the relevant expression for k_a^{os} then is[1]

$$k_a^{os} = 4\pi N_{Av}(r_p + r_M)(D_M + D_p)\frac{V^{os}}{V_p}\overline{f}_{el} \quad (5)$$

The equilibrium constant, K^{os}, for the outer-sphere reactant pair is defined in terms of the free metal ion concentration in the bulk solution, c_M^*. Under high charge density conditions,[1] K^{os} is simply related to the local potential ψ_p by Boltzmann statistics[15]

$$K^{os} = \frac{4}{3}\pi a^3 N_{Av} \exp(-\boldsymbol{U}_p) \quad (6)$$

where $\boldsymbol{U}_p = z_M F\psi_p/RT$. The same factor $\exp(-\boldsymbol{U}_p)$ applies to the equilibrium concentration of free M_{aq}^{z+} inside of the particle body (high charge density case).[10] The outer-sphere dissociation rate constant, k_d^{os}, follows from k_a^{os}/K^{os}

$$k_d^{os} = 3\frac{(r_p + r_M)}{a^3}(D_M + D_p)\frac{V^{os}}{V_p}\frac{\boldsymbol{U}_p}{1 - \exp(-\boldsymbol{U}_p)}$$

high charge density regime (7)

Electric Relaxation Times. Consider the case of M_{aq}^{z+} ($z > 1$) in a negatively charged soft NP dispersion containing excess 1:1 background electrolyte. The M_{aq}^{z+} will accumulate within the charged soft particle body to an extent determined by the overall effective Boltzmann equilibrium factor, $\overline{f}_B$. The $\overline{f}_B$ is the integral average of $f_B(r)$ over the HA particle volume for an assumed preset electric field (i.e., the setting of the field by the excess background electrolyte is considered complete).[14] The value of $\overline{f}_B$ represents the concentration ratio of the average free metal ion concentration in the particle body as compared to that in the bulk solution, $\overline{c_{M,p}}/c_M^*$. During the Boltzmann partitioning process, the concentration of M_{aq}^{z+} at the solution side of the particle/solution interface, c_M^0, increases with time t

$$\text{at} \quad t > 0: \quad c_M^0(t) = \frac{1}{\overline{f}_B}\overline{c_{M,p}}(t)$$

$$\text{as} \quad t \to \infty: \quad \overline{c_{M,p}}(t) = \overline{f}_B\, c_M^*$$

Overall, the evolution of c_M^0 with time can be described by[10]

$$c_M^0(t) = c_M^*[1 - \exp(-t/\tau_{rel})] \quad (8)$$

where τ_{rel} is the characteristic time constant for the soft particle 3D case with Boltzmann accumulation within the particle body

$$\tau_{rel} = \frac{r_p^2}{3(D_M + D_p)}\overline{f}_B \quad (9)$$

The average $\overline{f}_B$ applies over the whole transient because diffusion/distribution within the particle is considered to be infinitely fast. Thus, inside of the HA body, the concentrations of the outer-sphere associate M_{aq}^{z+}·S and free M grow exponentially with time according to a $[1 - \exp(-3(D_M + D_p)t/r_p^2\overline{f}_B)]$ dependence.[10] Therefore, compared to the case of complexation without accumulation, the conventional rate constant for diffusion to the sphere of radius r_p, $3(D_M + D_p)/r_p^2$, is modified by the factor $1/\overline{f}_B$.

Rate-Limiting Step in Overall Complex Formation. To establish whether the rate of diffusive supply of M_{aq}^{z+} to the particle or the inner-sphere complex formation is rate-limiting, we compare the limiting values of the pertaining rates of the two processes, $R_{a,p}$ and R_a^{is}, respectively. That is, $R_{a,p}$ is the overall rate, computed for full equilibrium between all M species inside of the particle, with steps 3 and 4 in Figure 1 at equilibrium, and R_a^{is} is the overall rate, computed for full ion partition equilibrium of M_{aq}^{z+} between the bulk solution and the particle,

dx.doi.org/10.1021/jp212226j | J. Phys. Chem. A 2012, 116, 6489−6496

with steps 1−3 at equilibrium ($c_{M,p} = \bar{f}_B c_M^*$). Direct comparison of the rates of diffusive supply and inner-sphere complex formation is done by expressing the rates in terms of the total concentration of reactive sites per unit volume of dispersion.

The limiting rate of diffusive supply, in the high charge density regime, can be given by[10]

$$R_{a,p} = 4\pi N_{Av}(r_p + r_M)(D_M + D_p)\bar{f}_{el}\, c_M^*\, c_S \ [\text{mol m}^{-3}\ \text{s}^{-1}] \tag{10}$$

where c_S is the smeared-out concentration of sites per unit of dispersion volume (mol m^{-3}). Strictly speaking, the applicable c_S in eq 10 is the concentration of free reactive sites S. As accumulation of M_{aq}^{z+} proceeds with time, the concentration of free S decreases, and $R_{a,p}$ will decrease and involve the equilibrium constants of steps 3 and 4. Thus, the $R_{a,p}$ computed from eq 10, where c_S is the total site concentration, represents the maximum diffusive supply rate, expressed as a rate of association between M and S.

The limiting rate of inner-sphere complex formation only, R_a^{is}, also expressed in terms of smeared-out concentrations, is given by the product of the rate constant of MS formation (generally that for dehydration of the metal ion, k_w) multiplied by the smeared-out concentration of outer-sphere complexes, $c_{M\cdot S}$, that is

$$R_a^{is} = k_w c_{M\cdot S} \tag{11}$$

According to the Fuoss−Eigen approach, the concentration of outer-sphere complexes is related to the intraparticulate concentration of free M_{aq}^{z+} via their stability constant K^{os}

$$K^{os} = \frac{c_{M\cdot S}}{c_{M,p} c_S} = \frac{4}{3}\pi a^3 N_{Av} \exp(-U_p) \tag{12}$$

where $\exp(-U_p) = \bar{f}_B$; this average Boltzmann factor applies at the location of site S. Combining eqs 11 and 12 yields

$$R_a^{is} = k_w V^{os} \bar{f}_B N_{Av} c_M^* c_S \tag{13}$$

from which we define

$$\overline{k_a^{is}} = k_w V^{os} \bar{f}_B N_{Av} \ [\text{m}^3\ \text{mol}^{-1}\ \text{s}^{-1}] \tag{14}$$

METHODS

Overall k_a for Cu(II)HA Complexes Derived from Experimental K^* and k_d^* Values. Humic substances are chemically heterogeneous, and thus, their effective thermodynamic and kinetic parameters depend on the degree of occupation of the reactive sites, θ. The total number of reactive sites, N_S, for each HA entity is not known, but as outlined in the Theory section, the differential K^* and k_d^* parameters are weighted averages which, for a given θ, to some extent, correspond to a particular type of binding site or to several site types with similar binding properties.[16] That is, with these differential parameters, in a sufficiently narrow range of θ values, to a first crude approximation, the number of operative reactive site types per HA entity can be set at unity.

The association rate constant, k_a, for MHA complexes may be derived from the experimentally determined values of both the differential equilibrium function, K^*, and the differential dissociation rate constant, k_d^* at a given θ. We have collated such values for a range of HA samples from the literature. The HA is derived from a variety of soil and peat sources, and no studies report both K^* and k_d^* values. Nevertheless, the general properties reported for the HA samples, for example, size and charge density, are broadly similar.

The K^* is defined by[16]

$$K^* = \frac{\sum_{i=1}^{n} K_i \theta_i (1 - \theta_i)\Delta\chi_i}{\sum_{i=1}^{n} \theta_i (1 - \theta_i)\Delta\chi_i} \tag{15}$$

where K_i is the equilibrium constant for complexes with site type i, θ_i is the degree of occupation of site type i by M, and $\Delta\chi_i$ is the mole fraction of site type i. Thus, at a given θ, K^* is controlled mainly by one type of site, that is, a small fraction of the total reactive sites that are near half-saturation. We have computed K^* values from published Cu/HA titration curves via[16]

$$K^* = \frac{-\alpha^2}{c_{Cu,t}}\left[\frac{1 - \frac{\alpha - 1}{\alpha}(\text{d ln } c_{HA,t}/\text{d ln } \alpha)}{1 + (\alpha - 1)(\text{d ln } \frac{c_{Cu,t}}{c_{HA,t}}/\text{d ln } \alpha)}\right] \tag{16}$$

where $\alpha = c_{Cu,t}/c_{Cu}^*$, $c_{Cu,t}$ is the total Cu(II) concentration in the dispersion, c_{Cu}^* is the free Cu^{2+} concentration in the bulk solution, and $c_{HA,t}$ is the total HA concentration expressed in any unit. It has been shown that, as a first approximation, there is a linear relationship between log θ and log K^*[17]

$$\log \theta = \text{const.} - \Gamma \log K^* \tag{17}$$

where Γ represents the degree of heterogeneity, and has a value between 0 and 1 ($\Gamma = 1$ corresponds to the homogeneous case).

For the derivation of the k_a values, it is necessary to use K^* values determined at the same pH and θ values and in the same ionic strength range as applicable for the k_d^* values (i.e., pH 7.5 and $I \approx 0.1$−0.01 mol dm^{-3}; see below). K^* values at pH 7.5 were obtained from a best fit line through the log K^* versus pH curves at a given θ. An example log K^* versus pH plot is shown in the Supporting Information for log $\theta = -2.0$, and the collated log K^* vs log θ plot applicable at pH 7.5 is given in Figure 2 for $I = 0.1$ and 0.01 mol dm^{-3}. The plots are linear

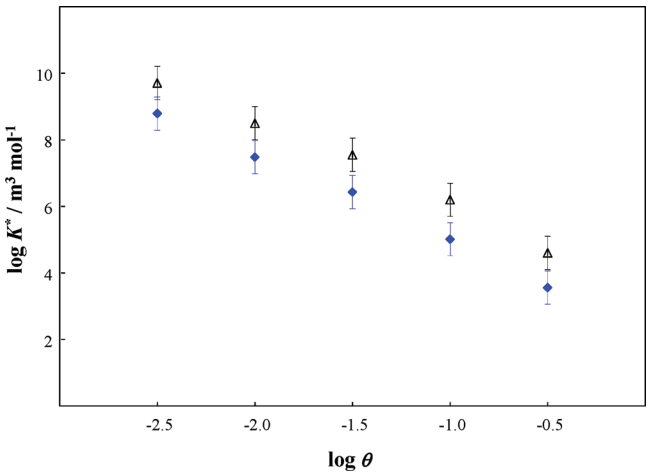

Figure 2. log K^* versus log θ at pH 7.5 for Cu complexes with soil and peat HA. Data correspond to ionic strengths of 0.1 mol dm^{-3} (blue ♦) and 0.01 mol dm^{-3} (△). The K^* values were computed on the basis of eq 16 from published titration curves.[18−26] Following usual practice, for computation of θ, the total concentration of the reactive sites is taken as the concentration of the carboxyl groups. The error bars correspond to the sum of the errors on the regression lines through the log K^* versus pH and the log K^* versus log θ data, that is, ±0.50 in log K^*.

dx.doi.org/10.1021/jp212226j | J. Phys. Chem. A 2012, 116, 6489−6496

as predicted by eq 17, and the slope yields $\Gamma \approx 0.4$, which corresponds to significant heterogeneity in the binding of Cu(II) by HA. Others have reported considerable heterogeneity in Cu complexation by HA.[18]

The k_d^* is defined by an expression analogous to that for K^*[27]

$$\frac{1}{k_d^*} = \frac{\sum_{i=1}^{n} \frac{1}{k_{di}} \theta_i(1-\theta_i)\Delta\chi_i}{\sum_{i=1}^{n} \theta_i(1-\theta_i)\Delta\chi_i} \quad (18)$$

The k_d^* values are measured by a ligand exchange approach. The starting point is an *equilibrated* dispersion of the metal ion plus HA, to which a strongly binding competing ligand is added in large excess to provoke dissociation of MHA. The rate of formation of complexes with the competing ligand is equated to the rate of dissociation of the HA complexes, and a k_d spectrum is fitted to the experimental data. The series of k_d^*,θ couples were obtained from the published kinetic spectra (proportion of bound metal as a function of the dissociation rate constant) by dividing the k_d abscissa into arbitrary segments with the corresponding surface area.

For the Cu(II)/HA system, the k_d^* values have been determined at pH 7.5 and ionic strength $\approx$ 0.1−0.01 mol dm^{-3} (Figure 3).[28] The overall quality of the plot is good, and

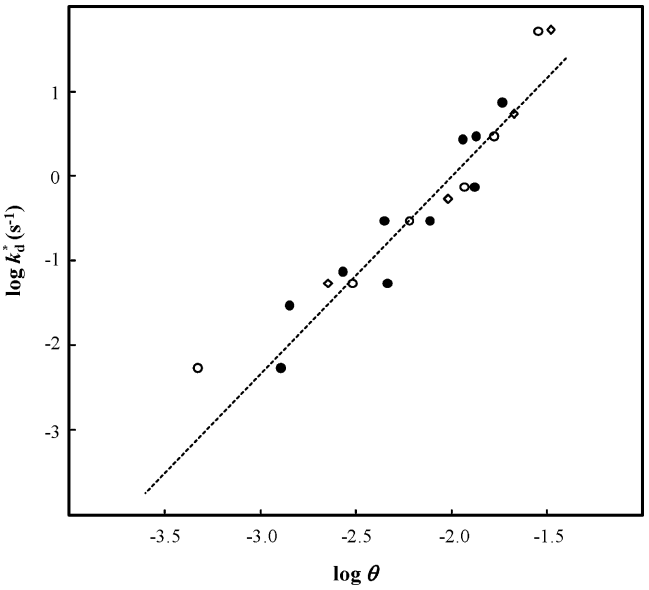

Figure 3. Log k_d^* versus log θ for Cu(II)−soil HA complexes. Points are derived from published kinetic spectra (proportion of bound metal as a function of the dissociation rate constant) and correspond to experimental data at pH 7.5 and pre-equilibration at ionic strengths of 0.2 (○), 0.02 (●), and 0.001 mol dm^{-3} (◊).[28] The dashed line is the best fit through the data points. The regression line through the log k_d^* versus log θ data gives a standard error of ±0.3 in log k_d^*.

the points for different ionic strengths are convincingly coincident. There is a bit of scatter around the best fit line, but this level of spread is typical of, and acceptable for, measurements on HA. The convergence of the data for the various pre-equilibration conditions suggests that in this low θ range, the assumption of a preset electric field is realistic.

To avoid significant extrapolation of the K^* and k_d^* values outside of the θ range under which they were determined, k_a values were derived within the log θ range of −2.5 to −1.5.

RESULTS AND DISCUSSION

Conductive Diffusion and Boltzmann Partitioning. The HA entities are small and thus cannot be considered as true Donnan particles for which the potential profile at the particle/solution interface is immaterial ($\kappa^{-1} \ll r_p$). The Donnan limit is approached by larger particles at high ionic strength (lowest κ^{-1}). The other extreme of small r_p and low ionic strength tends to the regime of an unscreened Coulombic f_{el}. For HA, the potential profile within the HA body is typically in the intermediate regime. The profile resembles a flattened bell shape, as shown in Figure 4. Further detail on computation

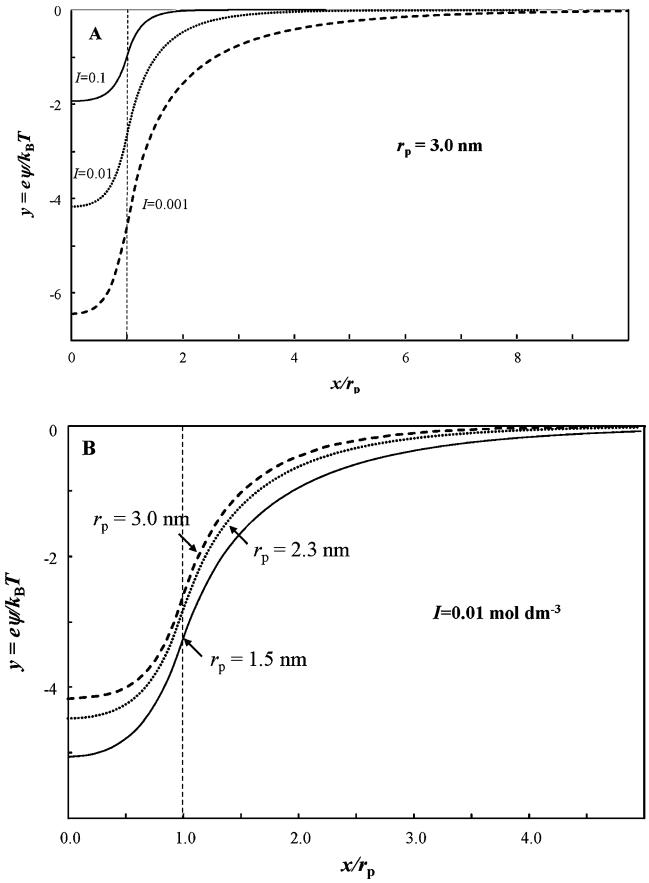

Figure 4. Potential profiles for HA particles. (A) r_p = 3.0 nm at I = 0.1 (solid curve), 0.01 (dotted curve), and 0.001 mol dm^{-3} (dashed curve). (B) r_p = 1.5 (solid curve), 2.3 (dotted curve), and 3.0 nm (dashed curve) at I = 0.01 mol dm^{-3}. The vertical dashed line corresponds to the particle/solution interface.

of the potential profiles from resolution of the nonlinear Poisson−Boltzmann equation is provided in refs 14, 29, and 30.

Typical values of particle radii, r_p, and intraparticulate space charge densities (fully dissociated carboxyl groups), ρ_o, for soil and peat HA samples considered herein are $r_p \approx$ 2.3−3.0 nm, with the corresponding $\rho_o \approx -10^2$ to -7×10^2 C m^{-3}, respectively.[8,9] Note that aquatic HA has an r_p of ∼1.5 nm and $\rho_o \approx -2 \times 10^2$ C m^{-3}. The computations of $\overline{f}_{el}$ and $\overline{f}_B$ are based on the electrostatic properties of the free HA in the background electrolyte ($\theta \rightarrow 0$).

We estimate the conductive acceleration of the diffusion rate of Cu^{2+}_{aq} on the basis of the effective $\overline{f}_{el}$ for a soft NP with a homogeneous charge distribution within the particle body

dx.doi.org/10.1021/jp212226j | J. Phys. Chem. A 2012, 116, 6489−6496

(see above).[14] Results are shown in Figure 5 for typical HA parameters.

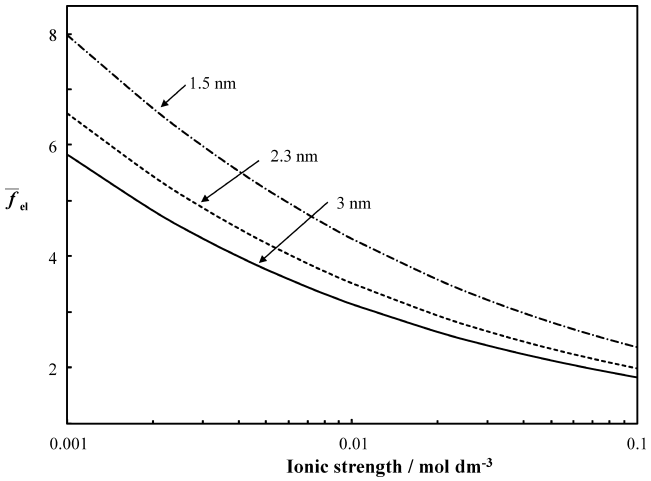

Figure 5. Plot of $\overline{f}_{el}$ versus ionic strength for HA and various values of the particle radius r_p. The curves correspond to r_p = 1.5 nm and ρ_o = -2×10^2 C m^{-3} (dot–dashed curve), r_p = 2.3 nm and ρ_o= -10^2 C m^{-3} (dashed curve), and r_p = 3 nm and ρ_o= -0.7×10^2 C m^{-3} (solid curve).

Likewise, the $\overline{f}_B$ is computed by integrating the local $f_B(r)$ over the HA particle volume using the preset potential distribution. Results are shown in Figure 6 for the same HA parameters as those used for the computation of $\overline{f}_{el}$.

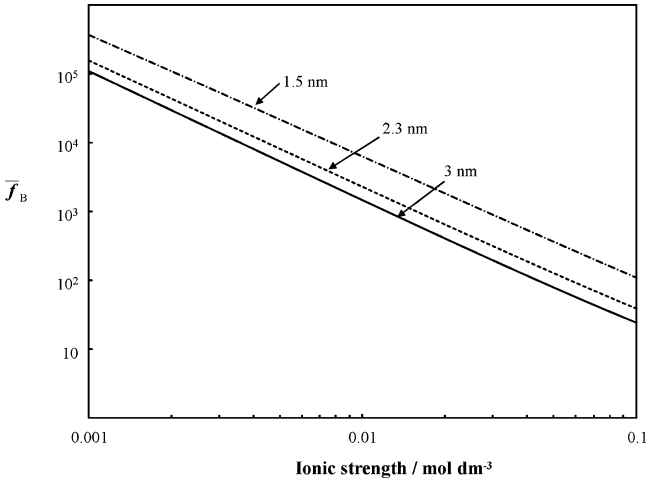

Figure 6. Plot of $\overline{f}_B$ versus ionic strength for HA with various values of the particle radius r_p. The curves correspond to r_p = 1.5 nm and ρ_o= -2×10^2 C m^{-3} (dot–dashed curve), r_p = 2.3 nm and ρ_o= -10^2 C m^{-3} (dashed curve), and r_p = 3 nm and ρ_o= -0.7×10^2 C m^{-3} (solid curve).

Figures 5 and 6 show that both $\overline{f}_{el}$ and $\overline{f}_B$ increase with decreasing ionic strength. For a HA particle with an r_p of 3 nm, $\overline{f}_{el}$ increases from ~2 at I = 0.1 mol dm^{-3} to ~6 at I = 0.001 mol dm^{-3}, while $\overline{f}_B$ increases more dramatically, from ~10 to 10^5, respectively. Overall, Figures 5 and 6 show that the Boltzmann equilibrium factor $\overline{f}_B$ significantly increases R_a^{is} (eq 13), and thus drastically reduces the ratio of the limiting rate of diffusive supply of M_{aq}^{z+} to the particle, $R_{a,p}$ (eq 10), relative to that for inner-sphere association R_a^{is} (eq 13), to an extent that increases with decreasing ionic strength. To a more modest extent, the coefficient for conductive acceleration $\overline{f}_{el}$ counteracts this reduction via the acceleration of the transport of the metal ion toward the particle. It should be stressed that the evaluation of $\overline{f}_{el}$ and $\overline{f}_B$ is based on the applicability of the mean-field Poisson–Boltzmann equation. It is likely that at sufficiently low electrolyte concentrations (0.001 mol dm^{-3}) where the inner particle potential reaches values as large as −100 to −150 mV (Figure 4), intricate electric phenomena, not included in the Poisson–Boltzmann theory, start to play a significant role in governing (i) the electric potential distribution inside and outside of the particle and (ii) the fundamentals of intraparticulate metal complexation at a level that goes beyond that of the Eigen-like mechanism. One may mention, for instance, the condensation of the counterions from background electrolyte on the structural charges carried by the humics, which results in a decrease of the effective particle charge density and thus a decrease of the intraparticulate field distribution. In addition, the effects related to orientation of water molecules at the particle/solution interphase, following strong double-layer field-mediated electrostatic polarization, are discarded within the continuous and structureless solvent framework of the Poisson–Boltzmann equation. Due to the current lack of knowledge for correctly predicting (on a *molecular* scale) the electrostatic features of heterogeneous nanoparticles like humics, it would be highly speculative to provide upper boundary values attainable by $\overline{f}_{el}$ and $\overline{f}_B$ that are fully consistent with the assumptions underlying the correctness in applying the mean-field approach adopted here. However, despite these limitations, the quantitative recovery of experimental electrophoretic mobility values of humics from the mean-field electrohydrodynamic formalism for soft nanoparticles[30] indirectly provides some confidence in the use of Poisson–Boltzmann theory within the 0.001–0.1 mol dm^{-3} range and thus in the order of magnitudes obtained for $\overline{f}_{el}$ and $\overline{f}_B$ (Figures 5 and 6). This confidence is further strengthened by this study that successfully deciphers the double-layer effects impacting the chemodynamics of Cu(II)–humics complexes (eqs 4 and 14), as detailed in the next section.

Relevant Rate-Limiting Processes Controlling the Experimental K^* and k_d^* Values. Identification of the rate-limiting step is made by comparing the k_a derived from the experimental K^* and k_d^* values (given in Figures 2 and 3; k_a = $K^* k_d^*$) with the computed rate constants in the limiting rate expressions, that is, $k_{a,p}$ from eq 4 and $\overline{k}_a^{is}$ from eq 14. For CuHA, the inner-sphere complex is sufficiently stable ($K_{int} c_S$ > 10^2 in the log θ range of −1.5 to −2.5), where K_{int} is the intrinsic stability constant for MS (=$K^*/\overline{f}_B$), so that all M entering the particle is practically converted to MS.

The experimentally derived k_a values, applicable at pH 7.5 and ionic strengths of 0.1 and 0.01 mol dm^{-3}, over a range of θ values, are compared with the computed $k_{a,p}$ and $\overline{k}_a^{is}$ values in Figure 7. Both $k_{a,p}$ and $\overline{k}_a^{is}$ increase with decreasing ionic strength. In the case of $\overline{k}_a^{is}$, a significant impact of ionic strength is observed due to the increase in $\overline{f}_B$ (Figure 6). For $k_{a,p}$, the increase in magnitude at lower ionic strength is more modest, in accord with the ionic strength dependence of $\overline{f}_{el}$ (Figure 5). For the range of θ values plotted, there is a very slight decrease in $k_{a,p}$ as a function of increasing θ, which reflects the decrease in the absolute magnitude of the particle potential due to the bound metal and hence a decrease in $\overline{f}_{el}$. For the range of θ values considered in Figure 7, there remains a large excess of free charged groups over bound metal ions. Under conditions where the extent of complexation results in practically complete

dx.doi.org/10.1021/jp212226j | J. Phys. Chem. A 2012, 116, 6489–6496

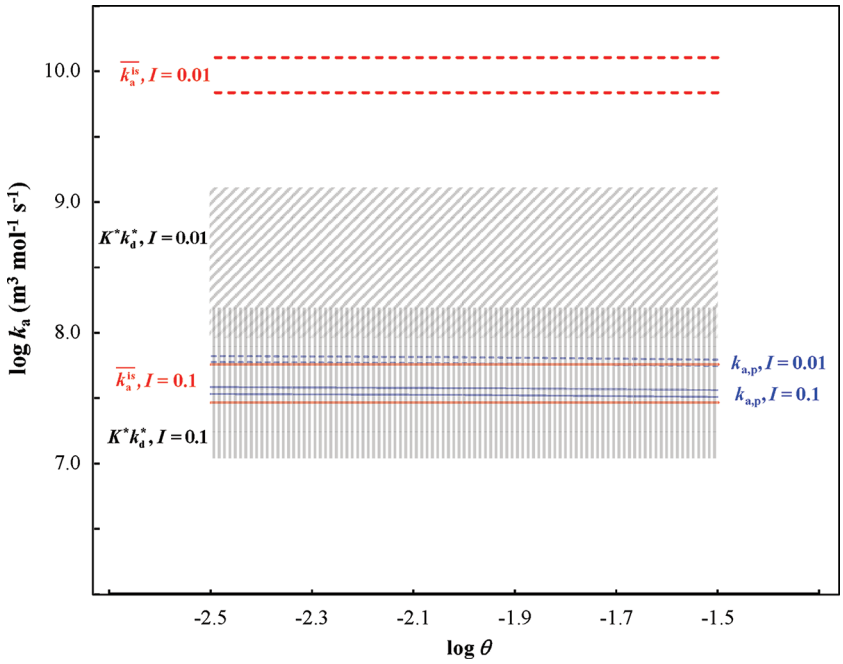

Figure 7. Overall k_a values for CuHA derived from experimental K^* and k_d^* data (shaded gray bands) as compared with the computed rate constants controlled by diffusive supply of metal ions, $k_{a,p}$ (blue horizontal lines), and inner-sphere complexation, $\overline{k_a^{is}}$ (red horizontal lines) (corresponding to the limiting rate expressions; see text for details). The results pertain to pH = 7.5 and I = 0.1 and 0.01 mol dm^{-3}. The band of computed $k_{a,p}$ values for each ionic strength covers the $\overline{f}_{el}$ range corresponding to r_p = 2.3−3.0 nm (solid blue lines, I = 0.1 mol dm^{-3}; dashed blue lines, I = 0.01 mol dm^{-3}). The band of $\overline{k_a^{is}}$ values for each ionic strength covers the $\overline{f}_B$ range for r_p = 2.3 nm and $\rho_o = -10^2$ C m^{-3} to r_p = 3.0 nm and $\rho_o = -0.7 \times 10^2$ C m^{-3} (solid red lines, I = 0.1 mol dm^{-3}; dashed red lines, I = 0.01 mol dm^{-3}). The bands for the experimental data include the estimated error (±0.6 log units) and correspond to I = 0.1 (vertical shaded gray band) and 0.01 mol dm^{-3} (diagonal shaded gray band). Other parameters: r_M = 0.45 nm, $D_{Cu} = 7.2 \times 10^{-10}$ m^2 s^{-1},[31] $D_p = 1 \times 10^{-10}$ m^2 s^{-1}.

charge compensation, the $k_{a,p}$ values for all ionic strengths converge to the diffusion-controlled limit.

Figure 7 shows that at an ionic strength of 0.1 mol dm^{-3}, the k_a derived from the experimental K^* and k_d^* values is comparable with both the computed rate constant controlled by the diffusive supply of M_{aq}^{z+} to the particle, $k_{a,p}$, and the rate constant controlled by inner-sphere complex formation, $\overline{k_a^{is}}$. Thus, the kinetics of the system are poised at conditions where $k_{a,p} \approx \overline{k_a^{is}}$. Upon decreasing the ionic strength to 0.01 mol dm^{-3}, the experimental k_a increases somewhat but remains closer to the lower computed rate constant, that is, $k_{a,p}$. Nevertheless, the increase in k_a upon lowering the ionic strength is greater than that computed for $k_{a,p}$, suggesting some persistence of mixed rate control. Furthermore, the k_a is found to be independent of θ, which confirms previous assumptions that the distribution in K^* is inversely reflected in that of k_d^*. This feature is manifest in the comparable absolute magnitude of the slopes of the plots of log K^* versus log θ (Figure 2) and log k_d^* versus log θ (Figure 3). Consistent results are obtained for this heterogeneous system for a range of θ values and at different ionic strengths, with various independent sources for the experimental values that pertain to different HA samples. Overall, the recently developed theory for chemodynamics of permeable charged nanoparticles[1,10,14] appears to provide a good description of Cu(II) complexation by HA.

CONCLUSIONS

The overall rate constant for association, k_a, is found to be independent of θ. This result is the first confirmation of previous assumptions that the distribution in the thermodynamic stability constant is reflected in that of the dissociation rate constant.[6,7] Our analysis of the chemodynamics of Cu(II) complexation by soil- and peat-derived HA shows that at an ionic strength of 0.1 mol dm^{-3}, both the diffusive supply of M_{aq}^{z+} to the particle and the rate of formation of the inner-sphere complex contribute to the observed overall rate of complex formation. Upon decreasing the ionic strength, the rate of inner-sphere complex formation is greatly enhanced, and consequently, the system moves toward the diffusive supply of metal ions being rate-limiting overall.

Our findings are highly significant for interpretation of the chemodynamics of metal complexation by HA and predictions of the lability of complex species. Current practice for deriving the kinetic parameters for humic complexes with a range of metal ions is to assume that the rate of inner-sphere complexation is rate-limiting and governed by the rate of metal dehydration, k_w.[32,33] For rapidly dehydrating metal ions, for example, $Cu(H_2O)_6^{2+}$ in the ionic strength range of 0.1−0.01 mol dm^{-3}, such an assumption leads to predicted dissociation rate constants (and hence predicted labilities of CuHA complexes) that are an order of magnitude too high. Even greater discrepancies arise at lower ionic strengths, for example, typical of fresh waters, where $\overline{f}_B$ becomes very large.

The results also highlight the importance of the nature of the experimental conditions under which the kinetic parameters are derived. The data analyzed here are based on experiments with pre-equilibrated CuHA dispersions in which ionic partition equilibria are fully established ($\overline{f}_B$ fully attained). If one starts from the opposite case, that is, following the rate of association of added Cu(II) with HA, then the characteristic time constant for setting up of the Boltzmann partitioning equilibrium of the reactant Cu^{2+} ion is included in the process. That is, the rate constant $k_{a,p}$ remains practically the same as that for an

dx.doi.org/10.1021/jp212226j | J. Phys. Chem. A 2012, 116, 6489−6496

uncharged entity of the same size, but the attainment of the eventual equilibrium with the charged HA requires an $\overline{f}_B$ times higher supply of metal ions.

■ ASSOCIATED CONTENT

Supporting Information

A plot of log K^* for Cu(II) complexation by HA as a function of pH at log $\theta = -2.0$. This material is available free of charge via the Internet at http://pubs.acs.org.

■ AUTHOR INFORMATION

Notes

The authors declare no competing financial interest.

■ ACKNOWLEDGMENTS

This work was performed within the framework of the BIOMONAR project funded by the European Commission's seventh framework program (Theme 2: Food, Agriculture and Biotechnology), under Grant Agreement 244405.

■ SYMBOLS AND ABBREVIATIONS

a	center-to-center distance of closest approach between a hydrated metal ion and a complexing site (m)
c_M^*	bulk concentration of free metal ion M_{aq}^{z+} (mol m^{-3})
c_M^0	concentration of M_{aq}^{z+} at the solution side of the particle/solution interface (mol m^{-3})
$c_{M,p}$	concentration of free metal ion M_{aq}^{z+} inside of the particle (mol m^{-3})
$c_{M\cdot S}$	smeared-out concentration of outer-sphere complexes M·S (mol m^{-3})
c_S	smeared-out concentration of reactive sites, S (mol m^{-3})
D_M	diffusion coefficient of the metal ion M_{aq}^{z+} (m^2 s^{-1})
D_p	diffusion coefficient of the particle (m^2 s^{-1})
$\overline{f}_B$	average Boltzmann equilibrium partitioning factor
f_{el}	average coefficient for conductive diffusion
Γ	degree of heterogeneity
k_a^{os}	rate constant for outer-sphere ion pair association (m^3 mol^{-1} s^{-1})
k_a^{is}	rate constant for inner-sphere complex formation from the precursor outer-sphere complex (s^{-1})
$\overline{k_a^{is}}$	overall association rate constant when inner-sphere complex formation is rate-limiting (m^3 mol^{-1} s^{-1})
k_a	overall rate constant for complex formation computed from experimental K^* and k_d^* values (m^3 mol^{-1} s^{-1})
$k_{a,p}$	overall formation rate constant when the diffusive supply of M_{aq}^{z+} to the particle is rate-limiting (m^3 mol^{-1} s^{-1})
k_d^{os}	rate constant for outer-sphere ion pair dissociation (s^{-1})
k_d^{is}	rate constant for inner-sphere complex dissociation (s^{-1})
k_d	overall rate constant for complex dissociation (s^{-1})
k_d^*	differential rate constant for complex dissociation (s^{-1})
k_w	rate constant for water substitution (s^{-1})
K^{os}	stability constant for the outer-sphere reactant pair (m^3 mol^{-1})
K^*	differential equilibrium function (m^3 mol^{-1})
κ^{-1}	Debye length (m)
l_C	separation distance between charged sites (m)
M_{aq}^{z+}	hydrated metal ion
N_S	number of potential binding sites in a particulate complexant
R_a^{is}	overall formation rate when inner-sphere complex formation is rate-limiting (mol m^{-3} s^{-1})
$R_{a,p}$	overall formation rate when diffusive supply of M_{aq}^{z+} is rate-limiting (mol m^{-3} s^{-1})
r_p	particle radius (m)
S	site that covalently binds a metal ion
U	dimensionless interaction energy between M_{aq}^{z+} and a simple ligand
U_p	dimensionless interaction energy between M_{aq}^{z+} in the bulk solution and that inside of the particle body
V^{os}	outer-sphere volume for an ion pair between M_{aq}^{z+} and individual site S (m^3)
V_p	particle volume (m^3)
τ_{rel}	characteristic time constant for electrostatic relaxation (s)
$\overline{\psi}_p$	average electrostatic potential difference between the solution and the particle body (V)

■ REFERENCES

(1) van Leeuwen, H. P.; Town, R. M.; Buffle, J. *Langmuir* **2011**, *27*, 4514.
(2) Poupko, R.; Luz, Z. *J. Chem. Phys.* **1972**, *57*, 3311.
(3) Sokol, L. S. W. L.; Fink, T. D.; Rorabacher, D. B. *Inorg. Chem.* **1980**, *19*, 1263.
(4) Powell, D. H.; Helm, K.; Merbach, A. E. *J. Chem. Phys.* **1991**, *95*, 9258.
(5) Lewis, W. B.; Alei, M. *J. Chem. Phys.* **1966**, *44*, 2409.
(6) van Leeuwen, H. P.; Buffle, J. *J. Electroanal. Chem.* **1990**, *296*, 359.
(7) Buffle, J.; Zhang, Z.; Startchev, K. *Environ. Sci. Technol.* **2007**, *41*, 7609−7620.
(8) Avena, M. J.; Koopal, L. K.; van Riemsdijk, W. H. *J. Colloid Interface Sci.* **1999**, *217*, 37.
(9) Saito, T.; Koopal, L. K.; Nagasaki, S.; Tanaka, S. *Colloids Surf., A* **2009**, *347*, 27.
(10) van Leeuwen, H. P.; Buffle, J.; Town, R. M. *Langmuir* **2012**, *28*, 227.
(11) van Leeuwen, H. P.; Buffle, J. *Environ. Sci. Technol.* **2009**, *43*, 7175.
(12) Debye, P. *Trans. Electrochem. Soc.* **1942**, *82*, 265.
(13) von Smoluchoswki, M. Z. *Z. Phys. Chem.* **1917**, *92*, 129.
(14) Duval, J. F. L.; van Leeuwen, H. P. *J. Phys. Chem. A* **2012**, DOI: 10.1021/jp209488v.
(15) Fuoss, R. M. *J. Am. Chem. Soc.* **1958**, *80*, 5059.
(16) Buffle, J.; Altmann, R. S.; Filella, M. *Anal. Chim. Acta* **1990**, *232*, 225.
(17) Buffle, J. *Complexation Reactions in Aquatic Systems: an Analytical Approach*; Ellis Horwood: Chichester, U.K., 1988.
(18) Benedetti, M. F.; Milne, C. J.; Kinniburgh, D. G.; van Riemsdijk, W. H.; Koopal, L. K. *Environ. Sci. Technol.* **1995**, *29*, 446.
(19) Robertson, A. P.; Leckie, J. O. *Environ. Sci. Technol.* **1999**, *33*, 786.
(20) Xue, H. B.; Sigg, L. *Aquat. Geochem.* **1999**, *5*, 313.
(21) Christl, I.; Milne, C. J.; Kinniburgh, D. G.; Kretzschmar, R. *Environ. Sci. Technol.* **2001**, *35*, 2512.
(22) Saito, T.; Nagasaki, S.; Tanaka, S.; Koopal, L. K. *Radiochim. Acta* **2004**, *92*, 567.
(23) Christl, I.; Metzger, A.; Heidmann, I.; Kretzschmar, R. *Environ. Sci. Technol.* **2005**, *39*, 5319.
(24) Gondar, D.; Iglesias, A.; López, R.; Fiol, S.; Antelo, J. M.; Arce, F. *Chemosphere* **2006**, *63*, 82.
(25) Kolokassidou, C.; Pasahlidis, I. *Radiochim. Acta* **2006**, *94*, 549.
(26) Vidali, R.; Remoundaki, E.; Tsezos, M. *Water, Air, Soil Pollut.* **2011**, *218*, 487.
(27) Filella, M.; Buffle, J.; van Leeuwen, H. P. *Anal. Chim. Acta* **1990**, *232*, 209.
(28) Stanley, B. J.; Topper, K.; Marshall, D. B. *Anal. Chim. Acta* **1994**, *287*, 25.
(29) Duval, J. F. L.; Ohshima, H. *Langmuir* **2006**, *22*, 3533.
(30) Duval, J. F. L.; Wilkinson, K. J.; van Leeuwen, H. P.; Buffle, J. *Environ. Sci. Technol.* **2005**, *39*, 6435.
(31) von Stackelberg, M. O.; Pilgram, M.; Toome, V. *Z. Elektrochem.* **1953**, *57*, 342.
(32) Jansen, R. A. G.; van Leeuwen, H. P.; Cleven, R. F. M. J.; van den Hoop, M. A. G. T. *Environ. Sci. Technol.* **1998**, *32*, 3882.
(33) Warnken, K. W.; Davison, W.; Zhang, H.; Galceran, J.; Puy, J. *Environ. Sci. Technol.* **2007**, *41*, 3179.